Malaysian Journal of Analytical Sciences, Vol 23 No 4 (2019): 682 - 689
DOI: https://doi.org/10.17576/mjas-2019-2304-15

MALAYSIAN JOURNAL OF ANALYTICAL SCIENCES
Published by The Malaysian Analytical Sciences Society
ISSN 1394 - 2506

PRELIMINARY INVESTIGATION OF LOW CURRENT FLASH SINTERING IN ZIRCONIA NANOPARTICLE COMPACT

(Kajian Awal Persinteran Kilat Arus Rendah dalam Nanopartikal Zirkonia Kompak)

Michiyuki Yoshida[1]*, Mitsuki Hada[1], Yutaka Shinoda[2], Osamu Sakurada[1], Fumihiro Wakai[2]

[1]Department of Chemistry and Biomolecular Science,
Gifu University, 1-1 Yanagido, Gifu-city 501-1193, Japan
[2]Laboratory for Materials and Structures,
Tokyo Institute of Technology, 4259 Nagatsuta Midori-ku Yokohama-city,226-8503, Japan

**Corresponding author: myoshida@gifu-u.ac.jp*

Received: 31 March 2018; Accepted: 17 April 2019

Abstract

Flash sintering is a newly developed technique to quickly densify conductive ceramics in the presence of an electric field. At a critical combination of field and temperature, densification takes place in a few seconds. In this paper, the feasibility of the densification in flash sintering with low current was investigated in the newly developed compact consisted of zirconia nanoparticles. Homogeneous microstructure with densely packing of nano-particles was successfully obtained by gel-casting of nano-suspension. The grain size and relative density of the sample flash sintered at 30 mA/mm^2 were 40.9 nm and 86.8%, respectively. The sample densified with limited grain growth in low current flash sintering. Although the full densification was not achieved in the present study, the effectiveness of the nanoparticle compact to reduce the current for the densification during flash sintering was shown by comparing the results reported in flash sintering with the coarser microstructure.

Keywords: zirconia, flash sintering, gel-casting

Abstrak

Pensinteran kilat merupakan satu teknik yang baru dibangunkan untuk mempercepatkan pemampatan seramik konduktif dalam kehadiran medan elektrik. Pada kombinasi kritikal antara medan dan suhu, densifikasi berlaku dalam beberapa saat. Dalam manuskrip ini, keberhasilan densifikasi dalam pensinteran kilat pada arus rendah telah dikaji dalam kompak yang baru dibangunkan terdiri daripada zirkonia nanopartikel. Struktur mikro homogen dengan pengisian padat partikel nano telah berjaya dihasilkan menggunakan acuan gel ampaian nano. Saiz butir dan ketumpatan relatif sampel bersinter pada 30 mA/mm^2 masing-masing adalah 40.9 nm dan 86.8%. Sampel telah dimampatkan dengan pertumbuhan butiran yang terhad di dalam arus pensinteran kilat yang rendah. Walaupun pemampatan penuh tidak dapat dicapai di dalam kajian ini, namun keberkesanan kompak nanopartikel untuk merendahkan aliran arus pemampatan ketika pensinteran kilat telah dapat dilihat dengan membandingkan hasil laporan pensinteran kilat ketika struktur mikro yang lebih besar dijalankan.

Kata kunci: zirkonia, pensinteran kilat, acuan gel

Introduction

Sintering refers to the process of firing and consolidating a body shaped from powder particle, and is originated from the fabrication of the pottery. During the sintering process, inter-particle pores in the green body are eliminated by atomic diffusion driven by capillary forces. A variety of sintering techniques, such as normal sintering, hot isostatic or uniaxial pressing has been applied in the production of ceramic materials. During the last

10–15 years, field assisted sintering (FAST) and microwave sintering have grown as a consequence of advantages including higher heating, cooling rates and lower sintering temperatures, compared with the traditional techniques. Quite recently, "Flash Sintering", as an extremely fast sintering method, has attracted much interest since it was first reported by Cologna et al. in 2010 [1]. In their original report, a DC electric field is applied to a sample (3 mol% Y_2O_3-stabilized ZrO_2) while it is heated in a conventional furnace and at a certain furnace temperature the densification takes place in a few seconds. Flash sintering has now been demonstrated with a wide range of different ceramics with submicron or micrometer scale microstructure [2-9].

One of the confirmed obstacles to achieve the industrialization of flash sintering is the homogeneous heating of the sample. In flash sintering, the final specimen temperature achieved, which can be expected to determine the extent of sintering, is controlled primarily by the limiting current in the power supply. However, too high a limiting current gives more scope for temperature gradients and catastrophic localization of the current[10]. For practical application of flash sintering, therefore, more sophisticated powder technology, which allow low currents to obtain the homogeneous heating of the sample. It is well known that the sinterability is expected to be improved for applying nanoparticles as a starting material. The green body consisted with nano-particles is expected to be densified by flash sintering with the homogeneous heating in low current.

Recently, our group successfully fabricated the densely packed green body by gel-casting of zirconia nano-suspension [11]. The initial compact prepared by the gel-casting in our study had the densely packed structure with a narrow pore size distribution. Almost fully dense sample with 99.5% of theoretical density was successfully obtained by the pressureless sintering at 1100 °C, which is 300 °C lower than that prepared by conventional process. In this work, the feasibility of the densification in flash sintering with low current was investigated in the newly developed zirconia nanoparticle compact.

Materials and Methods

In this study, the green body consisting of 3mol% yttria stabilized zirconia (3YSZ) nanoparticle was prepared by gel-casting. 3YSZ nano-suspension with the average particle size of 16 nm (MEL Chemicals Ltd., U.K.) was used as the starting material. The solids loading of the starting suspension measured by gravimetric analysis was 7.0 vol%. The as-received suspension with weak acidic pH of 2.7 was modified by adding tetra methyl ammonium hydroxide (Sigma-Aldrich, U.S.A) to pH 9.5 for the complete dissociation of citrate. Subsequently, 4.5 wt.% of triammonium citrate (99% purity, Kanto Chemical Co. Inc., Japan) was added as the dispersant. 0.6 wt.% of agarose (LM, Kanto Chemical Co. Inc., Japan) was added to the prepared suspension as the gelling agent. The zirconia suspension was heated before adding agarose and kept at a temperature of 80 °C in a closed vessel. The prepared suspension was casted to a plastic mold. After one week drying, the green body was calcined at the temperature of 650 °C for decomposing organic additions. The calcined sample with cylindrical shape was machined to have a dimension of φ4.5 mm×3.8mm for flash sintering.

The sample was sintered in a vertical split furnace fixed on a universal testing machine (AG-I, Shimadzu Co., Kyoto, Japan). The sample was initially heated in the furnace at a rate of 20 °C /min to 500 °C and then at 10 °C /min. A schematic illustration of the experimental setup for flash sintering is shown in Figure 1. Platinum electrodes on top and bottom of the sample ensured the application of the electrical field. These electrodes were maintained between alumina disks and specimen under a constant load of 10 N (~0.6 MPa). The constant electric field, E = 60 V cm^{-1} was applied by a commercial DC power source (ZX-400HN, Takasago Ltd, Kawasaki, Japan) from the start of heating. The current limit, at which the power supply switched from voltage control to current control, was set to 30 mA/mm^2, which was 4 times lower than the reported value of 120mA/mm^2 to reach the full densification in flash sintering with submicron microstructure [12]. The voltage across the Platinum electrodes and the current passing through the sample were measured using digital multimeters. After switching form voltage control to current control, the electric field was loaded on the sample for 10sec, and then the furnace was switched off to cool it down. Relative density of the flash sintered sample was calculated using Archimedes' method by taking 6.10 g/cm^3 as the theoretical density of tetragonal zirconia. Microstructure of the sample was observed from the fractured surfaces. The samples were coated with osmium and observed by scanning electron microscope (Model S4800, Hitachi Co., Japan). The equivalent circle diameter measured by the image analysis of SEM photographs was defined as the grain size.

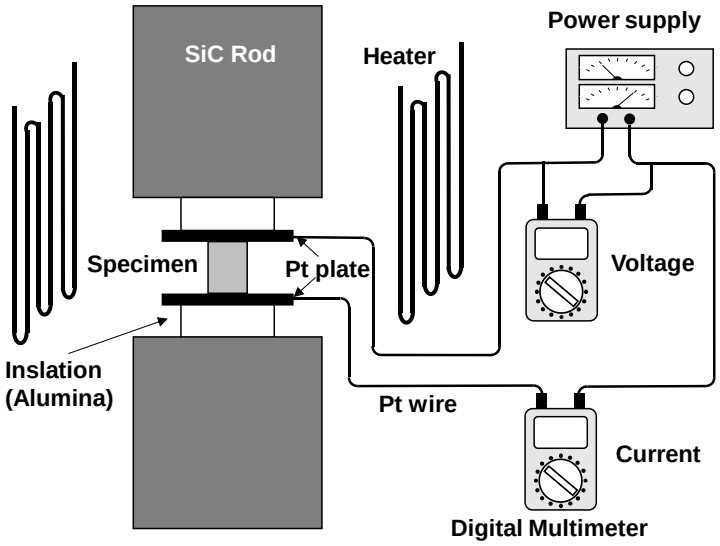

Figure 1. Schematic illustration of the experimental set up for flash sintering

Results and Discussion

Initial compact

The photograph of the gel-casted sample after drying is shown in Figure 2. After complete drying, no micro cracking and uniform shrinkage in a radial direction were observed. Figure 3 shows the FE-SEM micrograph for the fractured surface of the sample calcined at 650 °C. The grain size and relative density for the calcined sample were 28 nm and 52%, respectively. The calcined compact had a very narrow pore size distribution, and the average pore size was 15 nm. Homogeneous microstructure with densely packing of nano-particles was successfully obtained by slip-casting of nano-suspension.

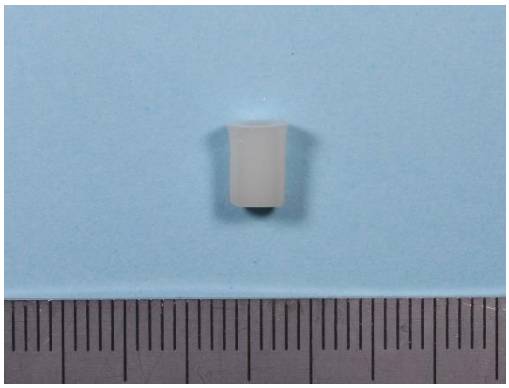

Figure 2. Photograph of the gel-casted sample

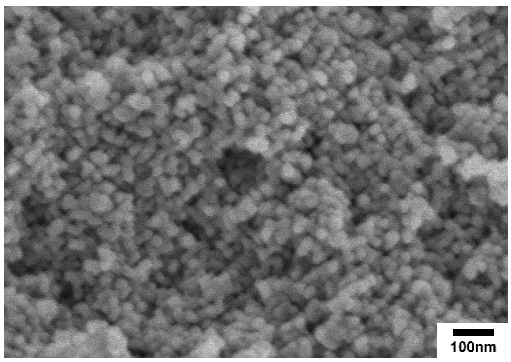

Figure 3. Fractured surface for the gel-casted sample calcined at 650 °C

General features of flash sintering

Current, voltage, resistance and power versus furnace temperature graphs during flash sintering are shown in Figure 4. The current rises slowly at first and then more rapidly until it reaches a pre-programmed limit (Figure 4(a)). The rapid increase in current at constant voltage shows that the specimen resistance was decreasing

throughout the process, as shown in Figure 4(c) so that the switch to current control results in a power spike (Figure 4(d)). These features demonstrate that the original results reported in the literature were successfully reproduced in this study. On the other hand, the observed width of the power spike in Figure 4(d) was about 150 sec, which was much longer than that reported in the literature (several seconds).

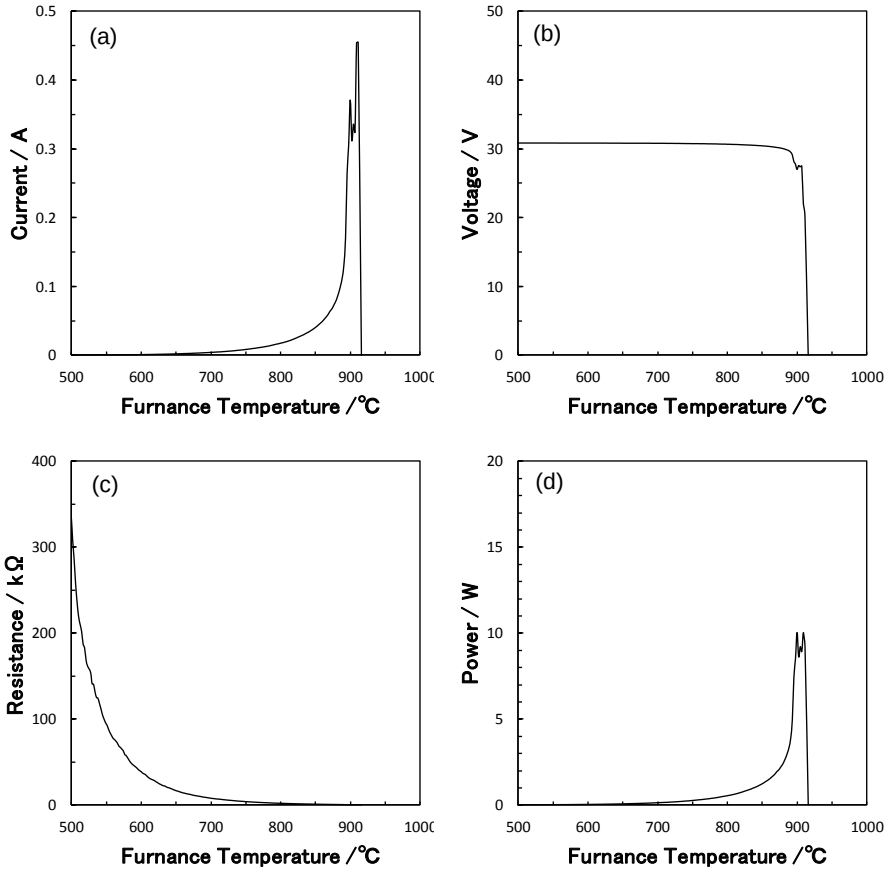

Figure 4. Current, voltage, resistance and power versus furnace temperature graphs during flash sintering

In the previous works, the connection between the electrodes and the specimen was made by inserting the electrodes through the holes in the specimens. This resulted in the improvement of the contact between the Pt and the specimen due to local melting/sintering around the contacts [13]. On the other hand, in this study, the contact between the electrodes and the sample was maintained by holding with SiC rods under a constant load of 10 N as shown in Figure 1. In this case, the rapid densification during flash sintering resulted in the poor contact between the electrode and the sample. This might cause an inhibiting effect on the runaway Joule heating and widen the width of the power spike in this study.

Specimen temperature and densification

The specimen temperature can rise considerably above the furnace temperature from Joule heating. We obtained an analytical estimate on the assumption of a uniform sample temperature, T_S, from the black body radiation model based on the Stefan-Boltzmann law [14]. According to this model, the sample temperature at steady state can be expressed as follows:

$$T_s = \left(T_0^4 + \frac{W}{A\varepsilon\sigma_s}\right)^{1/4} \quad (1)$$

where T_0 is the furnace temperature, W is the electrical power dissipated, A is the instantaneous surface area, ε is the emissivity and σ_s is Stefan–Boltzmann constant. The height of the specimens deduced from the displacement was used for calculating A in this case; it was assumed that the cross section of the specimen was constant during the test. The choice of emissivity is particularly problematic as it can be expected to vary with density during sintering as well as with surface roughness, wavelength and temperature. In this study, a value of 0.7 was chosen, based on the measurements of Tanaka et al. [15] on sintered zirconia. The relationship between the furnace temperature and the specimen temperatures calculated from eq. (1) are given in Figure 5(a). The dotted line in Figure 5(a) indicates the specimen temperature for no Joule heating, in which the specimen temperature is exactly same as the furnace temperature. The specimen temperature started to increase with Joule heating at around the furnace temperature of 600 °C, and then rapidly increased to reach 1270 °C at the furnace temperature of 880 °C. The displacement versus furnace temperature is shown in Figure 5(b), where the crosshead displacement was corrected with subtracting the thermal expansion of the SiC rods. The shrinkage of the specimen started to increase at the furnace temperature of 700 °C. The rapid densification was observed at the furnace temperature of 850 °C and was coincided with the rapid Joule heating of the sample apparently from Figure 5(a).

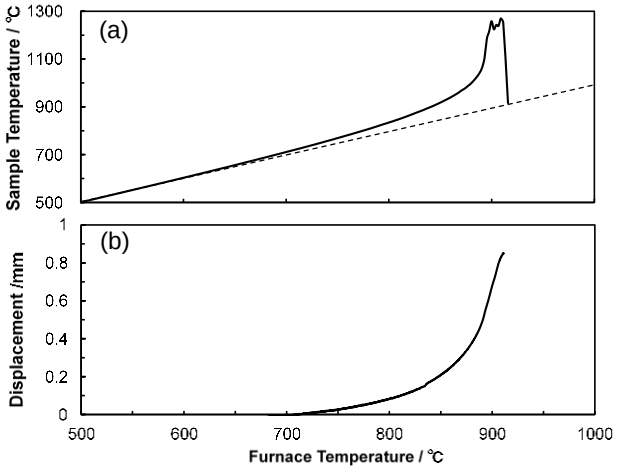

Figure 5. Sample temperature and displacement *vs* furnace temperature graphs during flash sintering

Microstructure

The micrograph for the fractured surface of the sample after flash sintering is shown in Figure 6. The grain size and relative density for the flash sintered sample were 40.9nm and 86.8%, respectively. In the case of the sample with submicron microstructure, the almost same density as in this study was obtained under the current of 60 mA/mm^2, which was twice as high as in this study [12]. This indicates that the nanoparticle compact reduces the current for the densification during flash sintering.

Average grain size is plotted as a function of density in Figure 7. For comparison, the results of normal sintering of gel casted sample [11], in which the samples were heated at the sintering temperatures for 2 hours, were also plotted in Figure 7. In normal sintering, the grain size increased with increasing the density. The hindered grain growth up to around 90% was shown in Figure 7. Subsequently, the exaggerated grain growth was observed at a density higher than 90% in which the relationship between grain size and relative density was parabolic. The transition from insignificant grain growth to rapid grain growth at around 90% density is believed to change from open to closed porosity, and this is the typical sintering behavior reported in the literature [16]. As shown in Figure 7, the result of flash sintered sample is in the region under a curve corresponding to the results of the normal sintering. This indicates that zirconia nanoparticle compact densified with limited grain growth in low current flash sintering.

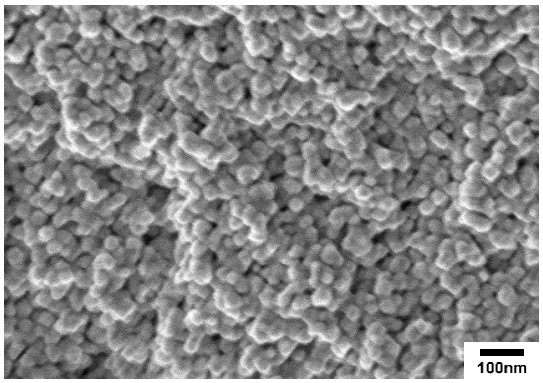

Figure 6. Fractured surface for the flash sintered sample at 30mA/mm^2

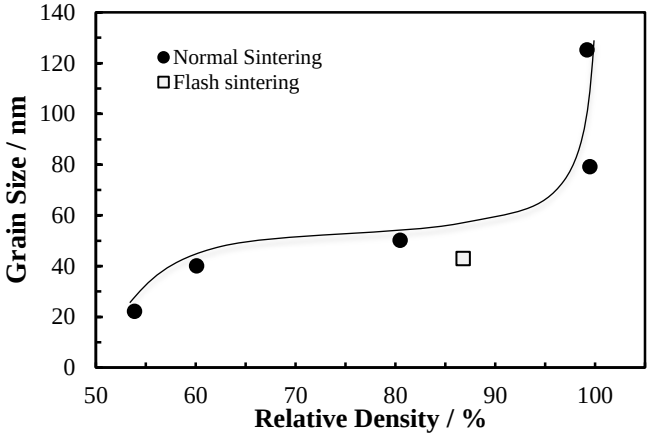

Figure 7. The relationship between relative density and grain size of the flash sintered sample. Results for normal sintered samples are plotted for comparison

The mechanisms responsible for flash sintering remain open to question [17, 18]. Recently, some researchers have shown that the power surge can be explained satisfactorily as thermal runaway resulting from the negative temperature coefficient of resistivity of most ceramics [10, 19, 20] whilst comparison with the sintering of powder compacts rapidly heated without an electric field suggests that the high densification rate may be at least in part a consequence of the fast heating in flash sintering [21]. Maximum heating rate observed in this study was 360 ◦C/min, which is 36 times higher than set up heating rate for the furnace, and comparable to that reported in the literature [21].

Although the full densification was not achieved, zirconia nanoparticle compact, obtained from gel-casting of nano-suspension, densified with the limited grain growth in low current flash sintering, and reduced the current for the densification during flash sintering. The optimization of the condition for the electrical loading, such as voltage and current set up in the power supply, is necessary to achieve the full densification of the nanoparticle compact.

Conclusion

In this study, we prepared the zirconia nanoparticle compact by gel-casting and demonstrated flash sintering. The conclusions obtained are summarized as follows: (1) Homogeneous microstructure with densely packing of nano-particles was successfully obtained by slip-casting of nano-suspension. The grain size and relative density of the

compact were 28nm and 52%, respectively. The sample had a very narrow pore size distribution with average pore size of 15nm, (2) While the original results reported in the literature were successfully reproduced in this study. the observed width of the power spike in this study was about 150 sec, which was longer than that reported in the literature (several seconds), (3) The grain size and relative density of the sample flash sintered at 30 mA/mm^2 were 40.9nm and 86.8%, respectively. The sample densified with limited grain growth in low current flash sintering. Although the full densification was not achieved in the present study, the effectiveness of the nanoparticle compacts to reduce the current for the densification during flash sintering was shown by comparing the result reported in flash sintering with the coarser microstructure.

Acknowledgement

This work was supported (in part) by the Collaborative Research Project of Materials and Structures Laboratory, Tokyo Institute of Technology.

References

1. Cologna, M., Rashkova, B. and Raj, R. (2010). Flash Sintering of Nanograin Zirconia in < 5 s at 850°C. *Journal of American Ceramic Society*, 93(11): 3556-3559.
2. Prette, A. L. G., Cologna, M., Sglavo, V. and Raj, R. (2011). Flash-sintering of Co_2MnO_4 spinel for solid oxide fuel cell applications. *Journal of Power Sources*, 196(4): 2061-2065.
3. Gaur, A. and Sglavo, V. M. (2014). Densification of $La0._6Sr_{0.4}Co_{0.2}Fe_{0.8}O_3$ ceramic by flash sintering at temperature less than 100 °C. *Journal of Material Sciences*, 49(18): 6321-6332.
4. Karakuscu, A., Cologna, M., Yarotski, D., Won, J., Francis, J. S. C., Raj, R. and Uberuaga, B. P. (2012). Defect structure of flash-sintered strontium titanate. *Journal of American Ceramic Society*, 95(8): 2531-2536.
5. Cologna, M., Francis, J. S. C. and Raj, R. (2011). Field assisted and flash sintering of alumina and its relationship to conductivity and MgO-doping. *Journal of European Ceramic Society*, 31(15): 2827-2837.
6. Muccillo, R. and Muccillo, E. N. S. (2014). Electric field-assisted flash sintering of tin dioxide. *Journal of European Ceramic Society*, 34(4): 915-923.
7. Zapata-Solvas, E., Bonilla, S., Wilshaw, P. R. and Todd, R. I. (2013). Preliminary investigation of flash sintering of SiC. *Journal of European Ceramic Society*, 33(13-14): 2811-2816.
8. Candelario, V. M., Moreno, R., Todd, R. I. and Ortiz, A. L. (2017). Liquid-phase assisted flash sintering of SiC from powder mixtures prepared by aqueous colloidal processing. *Journal of European Ceramic Society*, 37(2): 485-498.
9. Yoshida, H., Sakka, Y., Yamamoto, T., Lebrun, J. M. and Raj, R. (2014). Densification behaviour and microstructural development in undoped yttria prepared by flash-sintering. *Journal of European Ceramic Society*, 34(4): 991-1000.
10. Todd, R. I., Zapata-Solvas, E., Bonilla, R. S., Sneddon, T. and Wilshaw, P. R. (2015). Electrical characteristics of flash sintering: thermal runaway of Joule heating. *Journal of European Ceramic Society*, 35(6): 1865-1877.
11. Yoshida, M. Takeno, S. and Sakurada, O. (2016). Fabrication of translucent tetragonal zirconia by gelcasting of thin zirconia nano-slurry. *Journal of Ceramic Society of Japan*, 124(5): 500-505.
12. Francis, J. S. C. and Raj, R. (2013). Influence of the field and the current limit on flash sintering at isothermal furnace temperatures. *Journal of American Ceramic Society*, 96(9): 2754-2758.
13. Yoshida, M., Falco, S. and Todd. R. I. (2018). Measurement and modelling of electrical resistivity by four-terminal method during flash sintering of 3YSZ. *Journal of Ceramic Society of Japan*, 126(7): 579-590.
14. Raj, R. (2012). Joule heating during flash-sintering. *Journal of European Ceramic Society*, 32(10): 2293-2301.
15. Tanaka, H. Sawai, S., Morimoto, K. and Hisano, K. (2001). Measurement of spectral emissivity and thermal conductivity of zirconia by thermal radiation calorimetry. *Journal of Thermal Analytical Calorimetry*, 64(3): 867-72.
16. Mazaheri, C., Valefi, M., Hesabi, Z. R. and Sadrnezhaad, S. K. (2009). Two-step sintering of nanocrystalline $8Y_2O_3$ stabilized ZrO_2 synthesized by glycine nitrate process. *Ceramics International*, 35(1): 13-20.
17. Raj, R., Cologna, M., Francis, J. S. C. (2011). Influence of externally imposed and internally generated electrical fields on grain growth, diffusional creep, sintering and related phenomena in ceramics. *Journal of American Ceramic Society*, 94(7): 1941-1965.
18. Naik, K. S., Sglavo, V. M. and Raj, R. (2014). Flash sintering as a nucleation phenomenon and a model thereof. *Journal of European Ceramic Society*, 34(15): 4063-4067.

19. Zhang, Y. Y., Jung, J. I. and Luo, J. (2015). Thermal runaway, flash sintering and asymmetrical microstructural development of ZnO and ZnO–Bi_2O_3 under direct currents. *Acta Materialia*, 94: 87-100.
20. Bichaud, E., Chaix, J. M., Carry, C., Kleitz, M. and Steil, M. C. (2015). Flash sintering incubation in Al_2O_3/TZP composites. *Journal of European Ceramic Society*, 35(9): 2587-2592.
21. Ji, W., Parker, B., Falco, S., Zhang, J. Y., Fu, Z. Y. and Todd, R. I. (2017). Ultra-fast firing: Effect of heating rate on sintering of 3YSZ, with and without an electric field. *Journal of European Ceramic Society*, 37(6): 2547-2551.